

## Supplementary Information

Charge storage properties of ferromagnetic BaFe<sub>12</sub>O<sub>19</sub> and polypyrrole – BaFe<sub>12</sub>O<sub>19</sub> composites

Silin Chen and Igor Zhitomirsky\*

Department of Materials Science and Engineering, McMaster University,

1280 Main Street West, L8S 4L8, Hamilton, Ontario Canada

\*Email: zhitom@mcmaster.ca

Table S1. Capacitances, calculated from CV data.

Electrode	Capacitances $C_s$ ( $\text{F cm}^{-2}$ ) / $C_m$ ( $\text{F g}^{-1}$ ) at different sweep rates ( $\text{mVs}^{-1}$ )					
	<b>2 mVs<sup>-1</sup></b> $C_s$ ( $\text{Fcm}^{-2}$ ) $C_m$ ( $\text{Fg}^{-1}$ )	<b>5 mVs<sup>-1</sup></b> $C_s$ ( $\text{Fcm}^{-2}$ ) $C_m$ ( $\text{Fg}^{-1}$ )	<b>10 mVs<sup>-1</sup></b> $C_s$ ( $\text{Fcm}^{-2}$ ) $C_m$ ( $\text{Fg}^{-1}$ )	<b>20 mVs<sup>-1</sup></b> $C_s$ ( $\text{Fcm}^{-2}$ ) $C_m$ ( $\text{Fg}^{-1}$ )	<b>50 mVs<sup>-1</sup></b> $C_s$ ( $\text{Fcm}^{-2}$ ) $C_m$ ( $\text{Fg}^{-1}$ )	<b>100 mVs<sup>-1</sup></b> $C_s$ ( $\text{Fcm}^{-2}$ ) $C_m$ ( $\text{Fg}^{-1}$ )
BFO-E	0.146 3.650	0.159 3.963	0.160 3.988	0.159 3.974	0.153 3.823	0.147 3.670
HEBMBFO-E	1.00 24.88	0.91 22.90	0.83 20.80	0.73 18.35	0.58 14.55	0.44 11.05
BFO-GCA-E	0.319 7.97	0.313 7.84	0.308 7.71	0.301 7.54	0.285 7.12	0.265 6.63
HEBMBFO-GCA-E	1.34 33.51	1.27 31.73	1.19 29.82	1.10 27.49	0.94 23.52	0.75 18.69
PPy-NTS-E	4.53 129.38	3.59 102.50	2.81 80.36	2.03 58.00	1.04 29.75	0.61 17.29
PPy-PTS-E	4.66 133.26	4.17 119.03	3.66 104.48	3.03 86.47	1.97 56.32	1.18 33.65
BFO-PPy-NTS-E	2.61 65.19	2.17 54.37	1.86 46.47	1.54 38.54	0.99 24.86	0.57 14.16
BFO-PPy-PTS-E	2.82 70.45	2.74 68.43	2.62 65.62	2.42 60.52	1.88 46.93	1.26 31.38
HEBMBFO-PPy-NTS-E	3.39 84.71	3.00 75.03	2.68 67.11	2.38 59.48	1.78 44.60	1.09 27.27
HEBMBFO-PPy-PTS-E	3.21 80.26	3.01 75.36	2.75 68.76	2.30 57.55	1.35 33.72	0.70 17.55

Table S2. Capacitance calculated from CP data.

Electrode	Capacitances $C_s$ ( $\text{F cm}^{-2}$ )/ $C_m$ ( $\text{F g}^{-1}$ ) at different current density ( $\text{mA cm}^{-2}$ )			
	<b>3 mAcm<sup>-2</sup></b> $C_s$ ( $\text{F cm}^{-2}$ ) $C_m$ ( $\text{Fg}^{-1}$ )	<b>5 mAcm<sup>-2</sup></b> $C_s$ ( $\text{F cm}^{-2}$ ) $C_m$ ( $\text{Fg}^{-1}$ )	<b>7 mAcm<sup>-2</sup></b> $C_s$ ( $\text{F cm}^{-2}$ ) $C_m$ ( $\text{Fg}^{-1}$ )	<b>10 mAcm<sup>-2</sup></b> $C_s$ ( $\text{F cm}^{-2}$ ) $C_m$ ( $\text{Fg}^{-1}$ )
BFO-E	0.16 3.99	0.15 3.70	0.14 3.48	0.13 3.18
HEBMBFO-E	1.08 27.03	0.97 24.31	0.90 22.50	0.83 20.78
BFO-GCA-E	0.30 7.57	0.29 7.33	0.28 7.14	0.27 6.87
HEBMBFO-GCA-E	1.43 35.85	1.33 33.34	1.26 31.52	1.19 29.83
PPy-NTS-E	4.18 119.35	3.81 108.88	3.61 103.24	3.35 95.60
PPy-PTS-E	4.30 122.87	4.23 120.83	3.77 107.83	3.33 95.17
BFO-PPy-NTS-E	2.65 66.37	2.53 63.30	2.45 61.21	2.35 58.79
BFO-PPy-PTS-E	3.02 75.50	2.55 63.65	2.48 61.93	2.44 61.12
HEBMBFO-PPy-NTS-E	3.70 92.56	3.55 88.85	3.46 86.60	3.35 83.65
HEBMBFO-PPy-PTS-E	3.28 82.08	3.20 80.10	3.16 79.04	3.12 78.07

Table S3. EIS data for different electrodes

Electrode	$Z'$ at 10 mHz Ohm	$C'$ at 10 mHz $F\text{ cm}^{-2}$
BFO-E	47.90	0.033
HEBMBFO-E	113.95	0.061
BFO-GCA-E	13.86	0.124
HEBMBFO-GCA-E	65.41	0.117
PPy-NTS-E	2.33	2.55
PPy-PTS-E	1.36	2.89
BFO-PPy-NTS-E	2.51	1.62
BFO-PPy-PTS-E	1.40	2.08
HEBMBFO-PPy-NTS-E	1.56	2.09
HEBMBFO-PPy-PTS-E	2.01	1.88

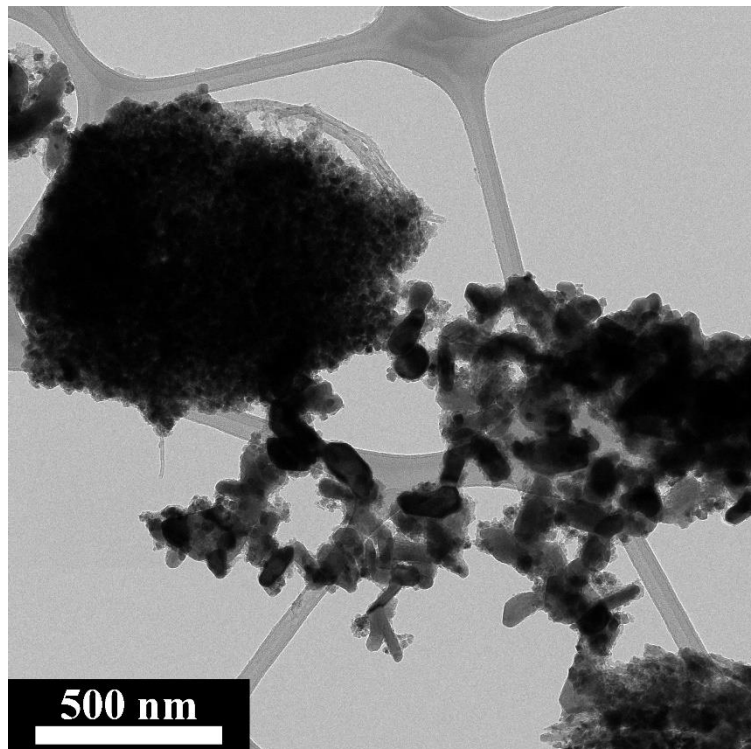


Figure S1. TEM image of as-received BFO obtained using TALOS L102C microscope (Thermo Fisher Scientific)

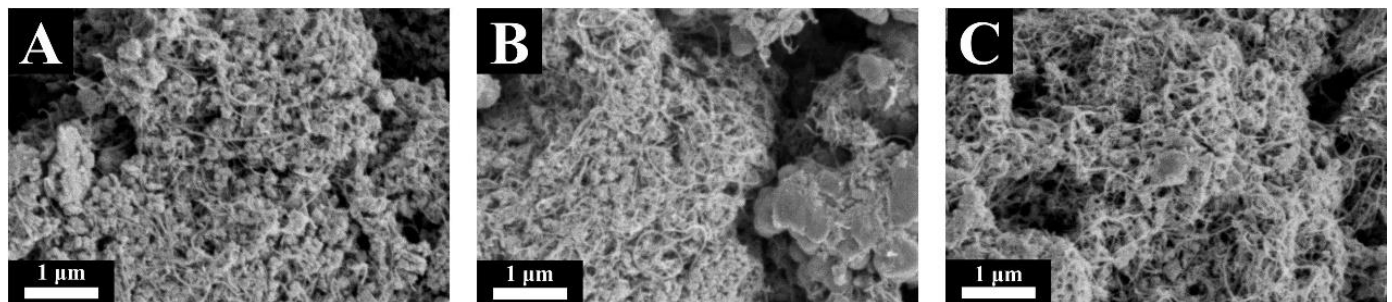


Figure S2. SEM images of (A) HEBMBFO-GCA-E, (B) HEBMBFO-PPy-NTS-E, and (C) HEBMBFO-PPy-PTS-E, obtained using Apreo 2 S LoVac microscope microscope (Thermo Fisher Scientific)

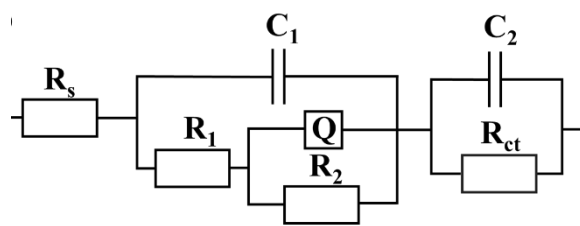


Figure S3. Equivalent circuit used for EIS data simulation[1]

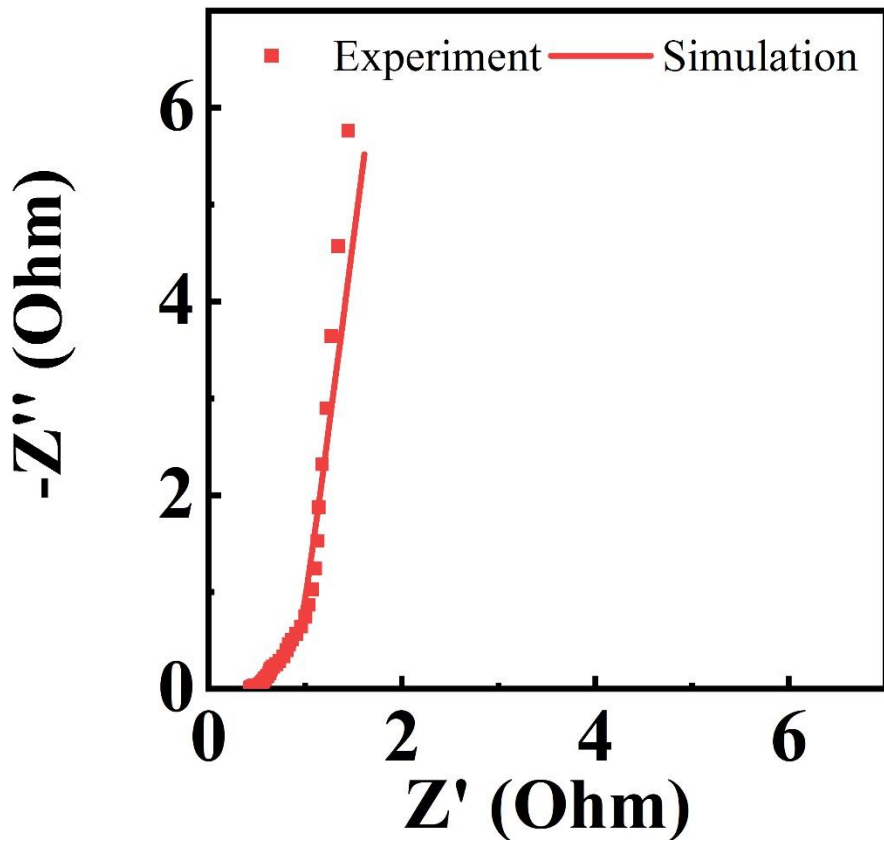


Figure S4. EIS data for HEBMBFO-PPy-NTS-E.

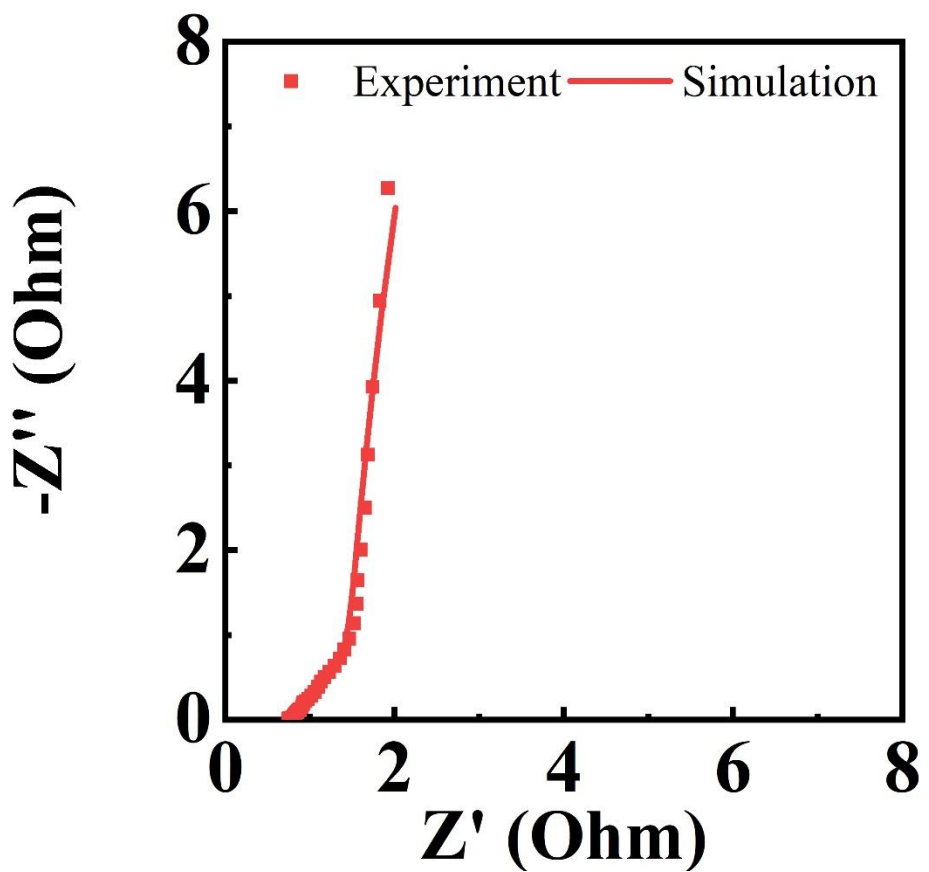


Figure S5. EIS data for HEBMBFO-PPy-PTS-E

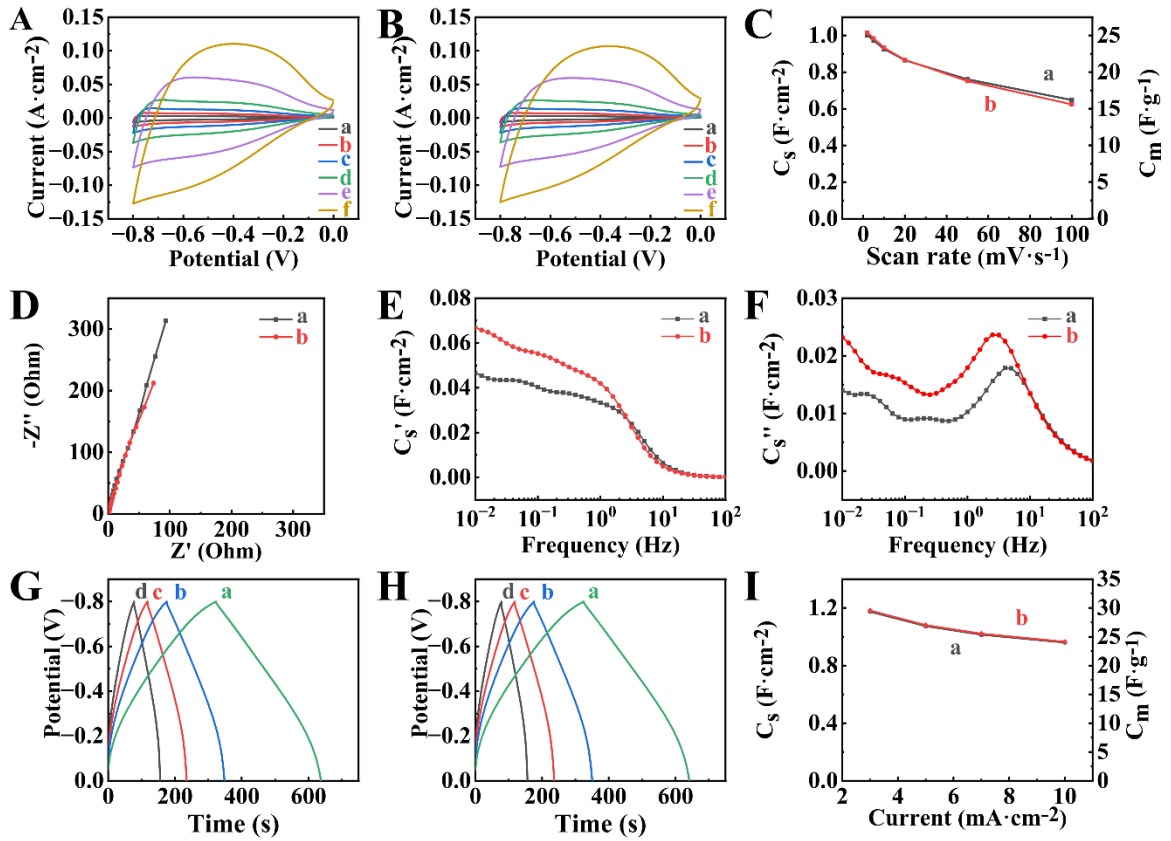


Figure S6. (A, B) CVs at sweep rates of (a) 2, (b) 5, (c) 10, (d) 20, (e) 50, and (f) 100  $\text{mV s}^{-1}$ , (C) capacitance calculated from CVs versus sweep rate, (D-F) EIS data, (G, H) CP data at current densities of (a) 3, (b) 5, (c) 7, and (d) 10  $\text{mA cm}^{-2}$  and (I) capacitance calculated from CP data versus current density for (A), (C(a)), (D(a)), (E(a)), (F(a)), (G), I(a) HEBM-BFO-NTS-E and (B), (C(b)), (D(b)), (E(b)), (F(b)). (H), I(b) HEBM-BFO-PTS-E.

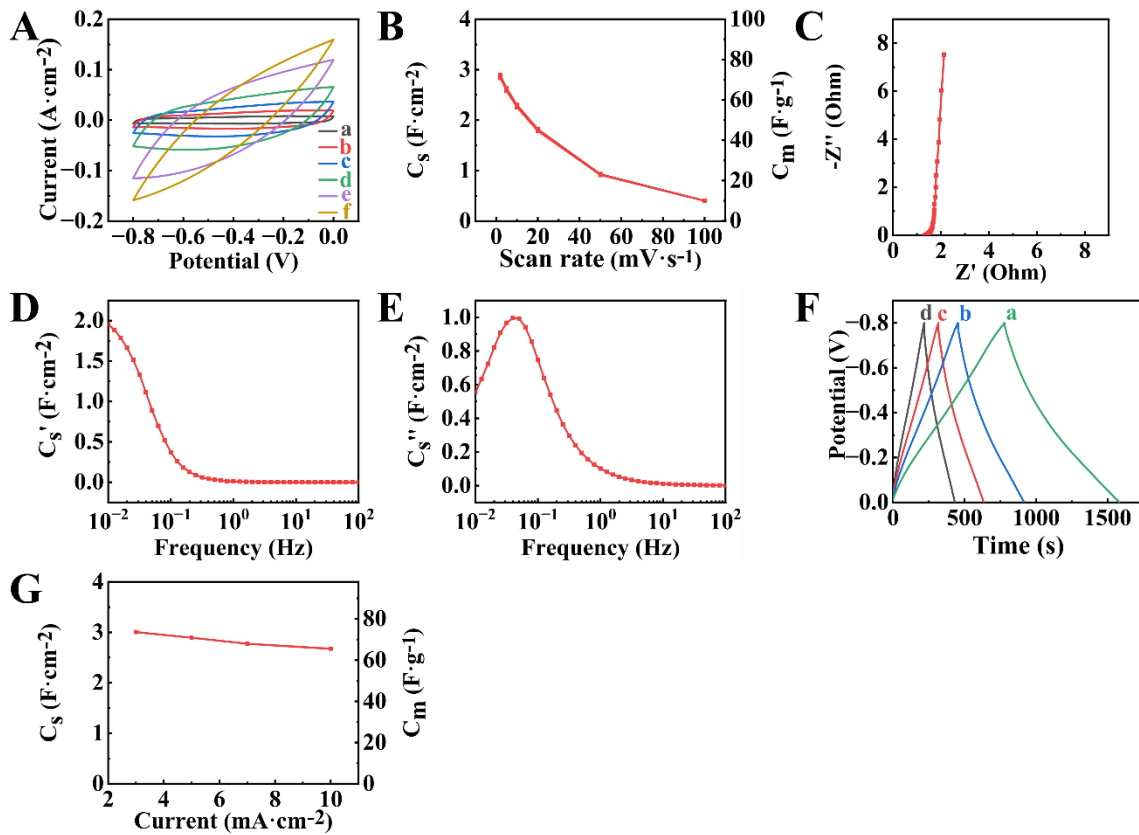


Figure S7 (A) CVs at sweep rates of (a) 2, (b) 5, (c) 10, (d) 20, (e) 50, and (f) 100  $\text{mV s}^{-1}$ , (B) capacitance calculated from CVs versus sweep rate, (C-E) EIS data, (F) CP data at current densities of (a) 3, (b) 5, (c) 7, and (d) 10  $\text{mA cm}^{-2}$  and (G) capacitance calculated from CP data versus current density for HEBM BFO-PPy-GCA-E.

[1] Y. Wang, Y. Liu, I. Zhitomirsky, Surface modification of MnO<sub>2</sub> and carbon nanotubes using organic dyes for nanotechnology of electrochemical supercapacitors, Journal of Materials Chemistry A 1(40) (2013) 12519-12526.